INDIRECT VS. DIRECT EFFECTS OF ANTHROPOGENIC SULFATE ON THE CLIMATE OF EAST ASIA AS SIMULATED WITH A REGIONAL COUPLED CLIMATE-CHEMISTRY/AEROSOL MODEL

FILIPPO GIORGI [1], XUNGQIANG BI [1] and YUN QIAN [2]

[1] *Abdus Salam International Centre for Theoretical Physics, Trieste, Italy*
[2] *Pacific Northwest National Laboratory, Richland, Washington, U.S.A.*

Abstract. We intercompare a series of multi-year simulations with a coupled regional chemistry-climate model for east Asia to assess the relative importance of direct and indirect (Type I) effects of anthropogenic sulfate on the climate of the region. Both direct and indirect aerosol effects induce a negative radiative forcing that results in a cooling of the surface and in a decrease of precipitation. Under present day sulfur emissions, the direct aerosol effects prevail during the cold season, while the indirect effects dominate in the warm season (when cloudiness is maximum over the region). When both the direct and indirect effects are included, the surface cooling varies in the range of –0.1 to over –1 K throughout the region and extended areas of statistically significant cooling are found in all seasons except winter. The indirect effects largely dominate in inhibiting precipitation, especially during the summer. When doubling the sulfur emissions, the direct effects are substantially strengthened, while the indirect effects are only marginally affected. This indicates that the indirect effects over the region might be asymptotically approaching their maximum efficiency. Overall, the indirect effects appear necessary to explain the observed temperature record over some regions of China, at least in the warm season. A number of uncertainties need to be addressed, such as due to Type II indirect effects, modeling of the relationship between aerosol concentration and cloud optical properties, and contribution of aerosols other than anthropogenic sulfate.

1. Introduction

The climatic forcing of atmospheric aerosols is due to what are traditionally referred to as 'direct' and 'indirect' effects (e.g., Haywood and Boucher, 2000; Penner et al., 2001; Ramaswamy et al., 2001): Direct effects are induced by the radiative forcing associated with the aerosol reflection and absorption of solar radiation; indirect effects are related to the role of aerosol particles as cloud condensation nuclei (CCN), since the CCN population determines the microphysical properties of clouds and thus affects the cloud optical properties and atmospheric residence time (e.g., Twomey et al., 1984; Charlson et al., 1992). The direct and indirect aerosol effects on climate have been extensively investigated, and a number of studies have shown that aerosols of anthropogenic origin can have significant climatic impacts, especially at the regional scale (e.g., Wigley, 1989; Charlson et al., 1990, 1992; Kiehl and Briegleb, 1993; Penner et al., 1994; Jones et al., 1994; Haywood et al., 1997; Myhre et al., 1998; Kiehl et al., 2000; Haywood and Boucher, 2000).

Climatic Change **58:** 345–376, 2003.

Anthropogenic aerosol effects are believed to be especially important over east Asia because of the rapid economic development of the region and the consequent increase in pollution emissions. Evidence of a possible anthropogenic aerosol signal in the observed climate record over China has been presented for example by Qian and Giorgi (2000). They observed a statistically significant cooling trend over the Sichuan Basin of southwest China in correspondence of increasing atmospheric aerosol optical thickness. A number of regional model studies have been recently carried out under the sponsorship of the CHINA-MAP project (Chameides et al., 1994, 1995) to elucidate the environmental and climatic impacts of rapid economic and industrial growth in China. These studies have followed two directions: first, the use of a comprehensive regional chemistry-transport model to investigate the effects of anthropogenic pollutants on agricultural productivity and air quality (Chameides et al., 1999a,b; Luo et al., 2000); second, the development of a coupled regional climate-chemistry/aerosol model to study the radiative forcing and climatic effects of anthropogenic aerosols (Qian and Giorgi, 1999; Qian et al., 2001; Giorgi et al., 2001).

In particular, Giorgi et al. (2002) (hereafter referred to as GBQ02) completed a series of multi-year regional simulations aimed at assessing the direct radiative forcing and climatic impact of anthropogenic sulfate and fossil fuel soot. Using observed emissions of anthropogenic sulfur dioxide, they found that the direct effects of anthropogenic sulfate and soot can induce a surface cooling of –0.1 to –0.7 K, highly variable at the subregional scale and statistically significant over some regions of China. However, although broadly consistent with the observed temperature trends over China, the signal due to the direct aerosol effects was not sufficient to explain the temperature signal implied by the observational record. Two of the factors identified by GBQ02 to explain this result were the lack of additional aerosols (e.g., carbonaceous particles and mineral dust, Chameides et al., 1999b) and the lack of indirect aerosol effects. To address the former issue GBQ02 performed a sensitivity experiment in which the sulfur emission was doubled compared to present day values. They found that the aerosol-induced cooling signal was substantially enhanced and it was statistically significant over broader areas of China. However, even with doubled sulfur emissions, the temperature response to the direct aerosol effects appeared smaller than that suggested by the observed temperature trend over some regions of China, particularly in the summer over south and southwest China.

In this paper we build on the work of GBQ02 and turn our attention to the contribution of the indirect effects of anthropogenic sulfate over the region. As suggested by Ramaswamy et al. (2001), the radiative forcing associated with the indirect aerosol effects is still characterized by a very high level of uncertainty. This is because of both the difficulty in modeling relevant processes and the lack of observational data to validate the models. Indirect aerosol effects can be of two types. In Type I, the aerosol-induced increase in CCN concentration leads to a reduction of the average cloud droplet radius which results in an increase

of the cloud reflectivity (Twomey et al., 1984). In Type II, the aerosol-induced change in cloud droplet size distribution affects the cloudwater-to-rainwater conversion mechanism, thereby changing (and generally increasing) the atmospheric residence time of clouds. Several parameterizations of Type I indirect effects are today available which relate the aerosol mass concentration to the cloud effective droplet radius and optical properties (e.g., Hegg, 1994; Boucher and Lohmann, 1995; Jones et al., 1994; Jones and Slingo, 1996). Such parameterizations have been used in a variety of modeling contexts (e.g., Haywood and Boucher, 2000). Concerning Type II effects, although some sensitivity studies have been carried out using simple parameterizations of the relationship between aerosol concentration and cloudwater-to-rainwater conversion efficiency (Lohmann and Feichter, 1997), the crudeness of the representation of cloud microphysics in climate models does not yet provide a robust enough framework to yield a realistic description of the processes involved. Based on these considerations, in the present work we limit our study to the role of Type I indirect effects.

A parameterization of Type I indirect aerosol effects was tested within a simple aerosol model coupled to a regional climate model by Qian and Giorgi (1999) in month-long simulations. They found that the relative magnitude of the direct and indirect aerosol radiative forcing depends substantially on the seasonal cloudiness conditions. In this work we implement the parameterization of Qian and Giorgi (1999) within the more sophisticated and realistic coupled regional climate-chemistry/aerosol model of Qian et al. (2001). In order to evaluate the relative role of direct and indirect effects of anthropogenic sulfate over China we then intercompare a series of multi-year simulations for the region under different sulfur emission scenarios. The intercomparison focuses on the aerosol radiative forcing and its effects on seasonally averaged surface air temperature and precipitation.

The primary limitation of this work is the lack of additional aerosols, such as carbonaceous particles and mineral dust, that are important over the region (Chameides et al., 1999b). Dust loadings are especially high over north China during the spring (Qian et al., 1999), so that the effects of dust may be limited to particular subregions and seasons. However, carbon particles are characterized by a more widespread distribution and are produced by different sources (e.g., Liousse et al., 1996). As described below, we crudely address this uncertainty by performing a sensitivity experiment in which the sulfur emission is doubled compared to present day emissions. Due to the different optical properties of sulfate and carbonaceous particles, this experiment has mostly an illustrative value, and we plan to study the role of additional aerosols with more comprehensive model simulations including different aerosol types.

2. Model and Experiment Design

2.1. CLIMATE MODEL AND SULFUR MODEL DESCRIPTION

The coupled regional climate-chemistry/aerosol model used in this work is extensively described by GBQ02 and references therein. The regional climate model component is the version of RegCM developed by Giorgi et al. (1993a,b) with some of the developments discussed by Giorgi and Shields (1999) and Giorgi et al. (1999), which include a prognostic equation for resolvable scale cloud water and a Kuo-type cumulus convection scheme. Radiative transfer is described using the radiation package of the NCAR Community Climate Model, version CCM3 (Kiehl et al., 1996), which describes the effect of different greenhouse gases (CO_2, CH_4, N_2O, CFCs), cloud ice and atmospheric aerosols. Cloud radiation is calculated in terms of cloud fraction and cloud water content, and a fraction of cloud ice is diagnosed by the scheme as a function of temperature.

The sulfur model is the same as described in detail by Qian et al. (2001) and is based on the model of Kasibhatla et al. (1997). It consists of prognostic equations for SO_2 and SO_4^{2-} which include transport by resolvable scale circulations and cumulus clouds, turbulent diffusion, dry deposition, wet removal by resolvable scale and cumulus precipitation, and chemical conversion from SO_2 to SO_4^{2-}. The parameterization of wet removal is based on the schemes of Giorgi and Chameides (1986) and Giorgi (1989) and depends on the local cloudwater-to-rainwater conversion rate, which is explicitly calculated for resolvable scale clouds and is specified for cumulus clouds. Below-cloud scavenging of SO_2 is also incorporated. Dry deposition of both SO_2 and SO_4^{2-} is parameterized using a constant deposition velocity with different values for land and ocean. Both gas-phase and aqueous phase SO_2-to-SO_4^{2-} chemical conversion pathways are included as described in Qian et al. (2001) and GBQ02. Note that our model also includes the effect of fossil fuel soot following the parameterization of Haywood et al. (1997) and Myhre et al. (1998), in which a constant soot-to-sulfate mass ratio of 0.075 is assumed. Given the small value of this ratio, however, the effect of fossil fuel soot is relatively small and the sulfate component largely dominates (see GBQ02).

The calculation of aerosol direct radiative forcing (see GBQ02) is based on the delta-Eddington representation used in the CCM3 radiation package (Kiehl et al. 1996), in which the aerosol radiative properties are described in terms of specific extinction, ψ_e, single scattering albedo, ω_o, and asymmetry parameter, g. Sulfate and fossil fuel soot are treated as an external mixture (see GBQ02), i.e. the optical properties for each aerosol type are treated separately. Optical properties for the sulfate are from the CCM3 radiative transfer scheme (Kiehl et al., 1996) while the fossil fuel soot optical properties are from Haywood and Shine (1997). The aerosol specific extinction also depends on the environmental relative humidity, *RH*.

The sulfur emission is from the database of Streets and Waldhoff (2000) and in the present experiments no seasonal variation of emission rate is included. Sulfur

emission over east Asia has a weak seasonal cycle, at most 20% difference between winter and summer (Smith et al., 2001) and therefore the use of an annually averaged emission facilitates the interpretation of simulated inter-seasonal differences. The spatial distribution of the emission is reported in Figure 1, and it shows maxima over the Sichuan Basin of southwest China (the region centered approximately at 30° N and 105° E), and over the coastal regions of east China. While this spatial distribution of the emission is kept constant in time, the magnitude of the emission rate increases from year to year based on the values given in Figure 1 of Qian and Giorgi (2000). Also shown in Figure 1 are two regions identified for more detailed analysis, a small region centered over the Sichuan Basin and a broader region of east China.

2.2. REPRESENTATION OF INDIRECT EFFECTS

Compared to the model of GBQ02, the present model includes the parameterization of Type I indirect effects described by Qian and Giorgi (1999). The scheme modifies the concentration of CCN, and hence the cloud properties, as a function of the aerosol mass concentration. In the CCM3 radiation package, cloud radiation is calculated in terms of two quantities, the cloud water content, L (g m^{-3}), and the effective cloud droplet radius r_e. The cloud water content is calculated by the model's explicit and cumulus cloud parameterizations (e.g., see Giorgi and Shields, 1999; and GBQ02). In the absence of anthropogenic aerosols, r_e is assigned the value of 10 μm, typical of clouds affected by a background CCN population (Briegleb, 1992).

Aerosol indirect effects are parameterized via a two-step approach (Jones and Slingo, 1996): in the first, a relationship is developed between the mass concentration of the sulfate aerosol and the number concentration of cloud droplets, N_c; the second step consists of a relationship between r_e and N_c. The first step is more difficult to quantify and it is the one that primarily contributes to the uncertainty in describing aerosol indirect effects. Jones and Slingo (1996) compared three methods for obtaining N_c from the sulfate concentration, i.e., those of Jones et al. (1994), Hegg (1994) and Boucher and Lohmann (1995). We selected the method of Hegg (1994) in which N_c is obtained as a function of the simulated sulfate mass mixing ratio via the formula

$$N_c = 90.7\ (\rho_a \times \chi)^{0.45} + 23. \tag{1}$$

where ρ_a is the density of dry air and χ is the sulfate mass mixing ratio. The advantage of this method is that it assumes that not all the atmospheric aerosol is sulfate, i.e., that a background non-sulfate aerosol is also present.

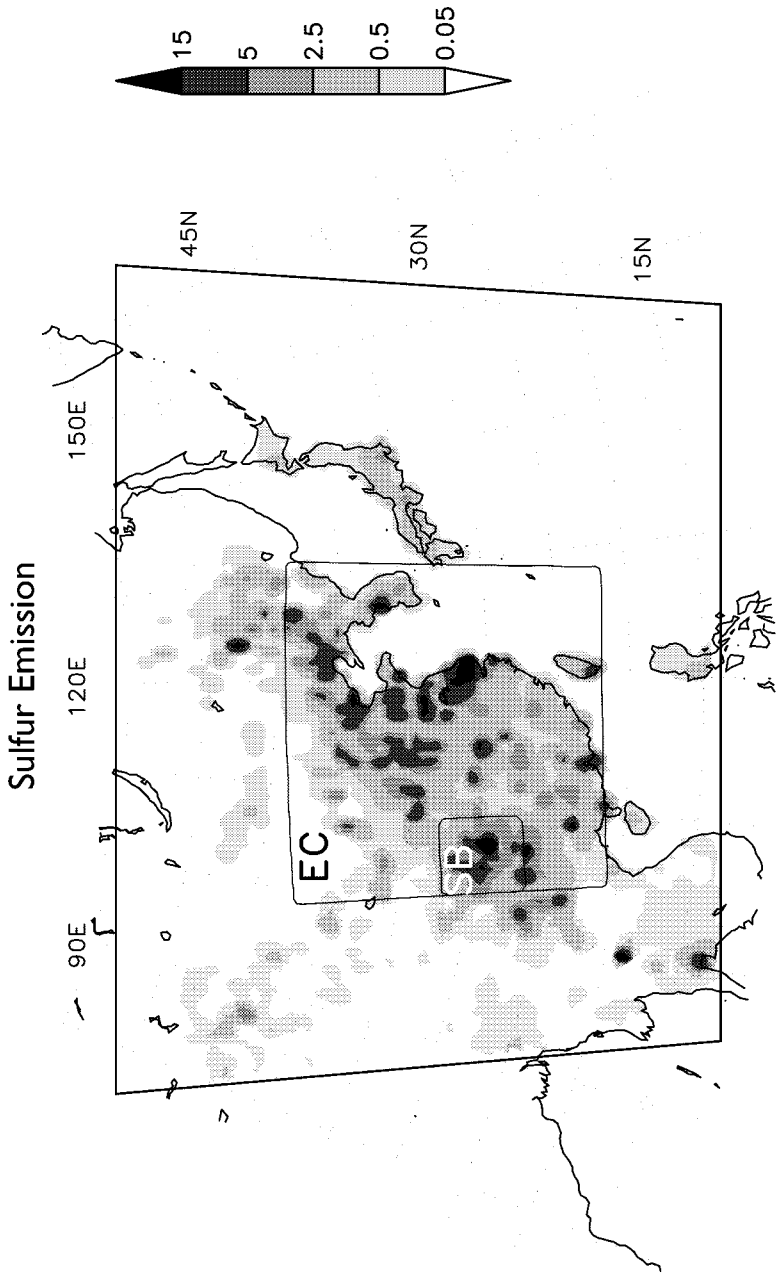

Figure 1. Distribution of sulfur ($SO_2 + SO_4^{2-}$) emission over East Asia for 1994 including both surface and high source (see text) (from Streets and Waldhoff, 2000). Units are g S m^{-2} yr^{-1}. The magnitude of the source changes year-by-year following the curve of Figure 1 of Qian and Giorgi (2000). Also shown are two subregions identified for more detailed analysis: east China (EC), which covers most of east China and the Korean peninsula; and a region encompassing the Sichuan Basin (SB). Note that the SB region is not included within the EC region.

Once N_c is calculated from Equation (1), the cloud water effective radius is calculated as a function of N_c and the cloud water content L via the relationship (Martin et al., 1994)

$$r_e = \left(\frac{3L}{4\pi \rho_w k N_c} \right)^{1/3}, \tag{2}$$

where ρ_w is the density of water and k is the cube of the ratio of the mean volume radius and the effective radius of the cloud-droplet spectrum.

2.3. SIMULATION DESIGN

The domain used in the simulations is the same as in GBQ02, which was also previously used for the CHINA-MAP project (e.g., Giorgi et al., 1999), and it encompasses most of east Asia and adjacent ocean waters at a grid point spacing of 60 km. The 5-year simulation period extends from January 1, 1993, to December 31, 1997. The large scale meteorological boundary conditions necessary to run the model are obtained from 6-hourly analyses of observations from the European Centre for Medium-Range Weather Forecast (ECMWF). Our analysis of the results is carried out on the averages over the five simulated years for the four seasons of December-January-February (DJF), March-April-May (MAM), June-July-August (JJA) and September-October-November (SON).

A set of five experiments for the full simulation period are intercompared in this paper. In the first, or control experiment (CONT), the sulfur model is run within the RegCM, but the aerosol is not radiatively active. In experiment DIR1 the direct sulfate and soot radiative forcing is included and the sulfur emission is the same as in CONT. In experiment IND1, the indirect forcing is accounted for along with the direct forcing within the model configuration of experiment DIR1. Finally, in experiments DIR2 and IND2 the model configuration is the same as in DIR1 and IND1, respectively, but the aerosol source is doubled compared to the control run. Note that our experiments DIR1 and DIR2 correspond to experiments DIRC1 and DIRC2 of GBQ02.

The DIR2 and IND2 experiments were conducted for two reasons. First, Chameides et al. (1999b) estimate the effects of additional aerosols by multiplying the sulfate optical depth by a factor of 2. Second, emissions from fossil fuel combustion in China are expected to increase in the next decades due to economic development. Streets and Waldhoff (2000) estimate that sulfur emissions over China might more than double by 2020, and Wang (1997) estimates an increase of sulfur emissions of a factor of $\sim$1.8 by 2020 compared to 1990. Therefore, the DIR2 and IND2 sensitivity experiments can be considered to either crudely represent the effects of additional aerosols or to describe possible future increases in sulfur emissions.

Our analysis primarily focuses on the comparison of the experiments IND1 and IND2 with the other experiments in order to isolate the indirect aerosol effects and compare them with the direct effects.

3. Results

An analysis of the CONT experiment and of the basic climatology of the RegCM for this simulation is presented by GBQ02 with reference to Giorgi et al. (1999). They show that the model reproduces the basic climatology of the region, which evolves seasonally from cold and dry winters to warm and wet summers through the onset and development of the east Asia monsoon. The main problems in the simulation are a cold temperature bias of a few degrees during the winter and a tendency of the model to overestimate precipitation by 10–25%.

A detailed discussion of the model sulfur cycle is reported by Qian et al. (2001) and GBQ02, who provide an extensive comparison of the different components of the SO_2 and SO_4^{2-} budgets with some available observations and with previous global model experiments. They find that the simulated sulfate burden shows magnitude and spatial structure in line with previous model studies, although with greater spatial variability, (e.g., Kasibhatla et al., 1997; Barrie et al., 2001) and is consistent with the observed spatial distribution of aerosol optical depths (e.g., Qian and Giorgi, 2000). The SO_2 budget is dominated by the aqueous phase chemical conversion to SO_4^{2-} and by the loss due to dry deposition, while the SO_4^{2-} budget is dominated by the source from aqueous phase chemical conversion of SO_2 and by the wet removal due to resolvable scale and cumulus cloud precipitation.

3.1. SIMULATION WITH PRESENT DAY SULFUR EMISSIONS

Figure 2 illustrates the average sulfate burden distribution in the IND1 experiment for DJF and JJA, while Tables I and II report the average seasonal burdens over the two regions of Figure 1. The burden in the primary plume varies in the range of 1 mg S m^{-2} to over 10 mg S m^{-2}. In both seasons the plume is elongated in a northeastward direction, during the summer because of the southwesterlies associated with the monsoon circulations, and during the cold season because of the mid-latitude westerlies and low latitude easterlies. A pronounced maximum in aerosol burden is found over the Sichuan Basin of southwest China, with secondary maxima over the coastal regions of central and northeast China. This maximum, which is consistent with observations of aerosol optical depth (see Qian et al., 2001), is due to the fact that the Sichuan Basin is an area of maximum emission and relatively stagnant meteorological conditions.

The sulfate burden is essentially determined by the balance of the source from SO_2-to-SO_4^{2-} gas-to-particle conversion and the sink due to wet removal. Both these processes are maximum in the summer and minimum in the winter, so that they tend to compensate, and thus to reduce the seasonality of the burden. Figure 2 and Tables I and II show that, when looking at the whole east China region, the burden is maximum in JJA and minimum in DJF. This is however not true everywhere. In fact, Table II shows that over the Sichuan Basin the minimum burden occurs in MAM. This is due to an increased efficiency of removal by precipitation

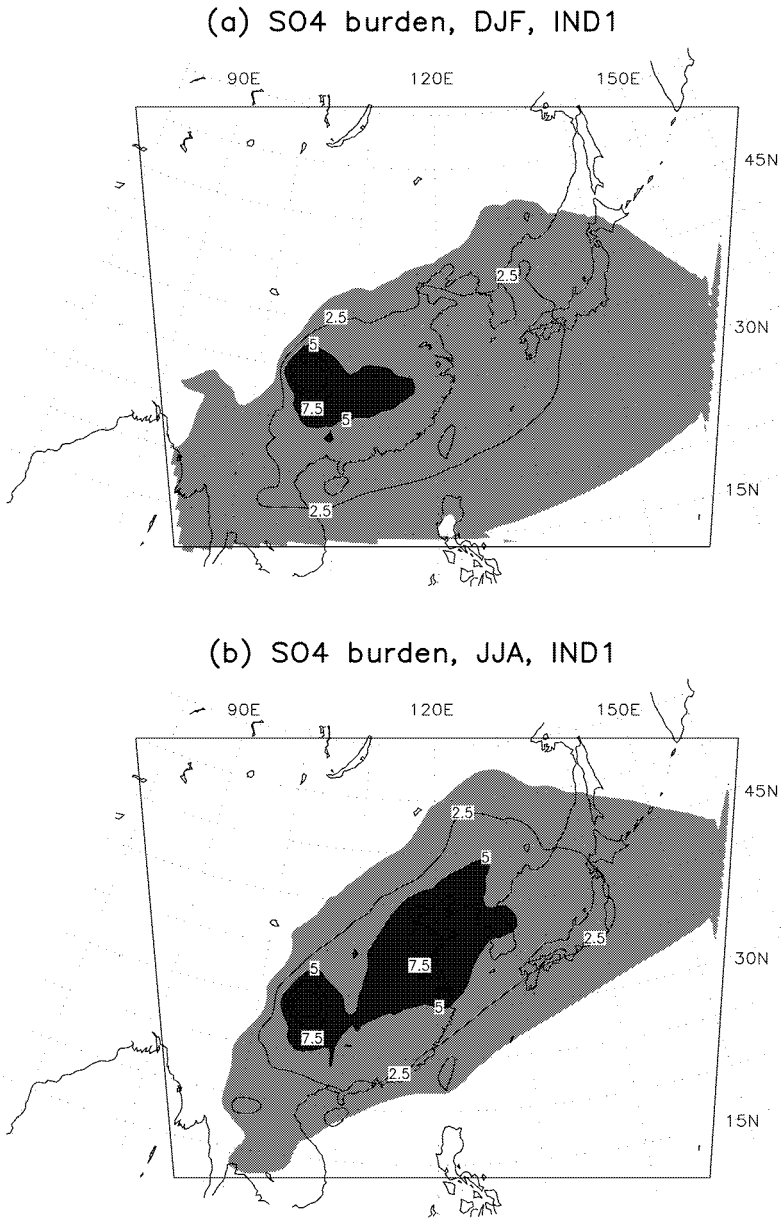

Figure 2. Simulated average SO_4^{2-} column burden in the IND1 experiment. (a) DJF; (b) JJA. Units are mg S m^{-2}. Light shading indicates burden greater than 1 mg S m^{-2}, dark shading indicates burden greater than 5 mg S m^{-2}.

Table I

Average sulfate burden (SO_4^{2-}) and difference in average TOA radiative forcing (ΔRF), cloud effective radius (r_e), surface air temperature (ΔT) and precipitation (ΔP) over the east China region (land points only, see Figure 1) between the experiments including the aerosol forcing and the control experiment. The units of ΔP are % of control precipitation

	DJF	MAM	JJA	SON
SO_4^{2-} (mg m^{-2})				
CONT	2.76	2.93	3.91	3.22
DIR1	2.73	2.92	3.83	3.19
IND1	2.72	2.97	3.87	3.20
DIR2	5.41	5.89	7.78	6.43
IND2	5.37	5.97	7.87	6.42
ΔRF (W m^{-2})				
DIR1-CONT	–2.29	–2.41	–2.65	–2.74
IND1-CONT	–3.93	–7.08	–11.77	–5.57
DIR2-CONT	–3.91	–4.50	–5.01	–4.90
IND2-CONT	–5.61	–9.15	–14.62	–7.55
Δr_e (μm)				
IND1-CONT	–2.10	–1.64	–2.02	–2.00
IND2-CONT	–2.31	–1.83	–2.24	–2.21
ΔT (K)				
DIR1-CONT	–0.21	–0.14	–0.07	–0.22
IND1-CONT	–0.39	–0.37	–0.42	–0.39
DIR2-CONT	–0.39	–0.28	–0.20	–0.34
IND2-CONT	–0.57	–0.53	–0.49	–0.54
ΔP (%)				
DIR1-CONT	–5.89	–2.25	–1.74	–4.19
IND1-CONT	–12.61	–7.87	–5.31	–9.85
DIR2-CONT	–10.01	–5.01	–4.80	–7.51
IND2-CONT	–16.61	–10.69	–7.30	–13.17

Table II

Average sulfate burden (SO_4^{2-}) and difference in average TOA radiative forcing (ΔRF), cloud effective radius (r_e), surface air temperature (ΔT) and precipitation (ΔP) over the Sichuan Basin (see Figure 1) between the experiments including the aerosol forcing and the control experiment. The units of ΔP are % of control precipitation

	DJF	MAM	JJA	SON
SO_4^{2-} (mg m^{-2})				
CONT	7.65	5.87	7.46	7.45
DIR1	7.62	5.98	7.42	7.54
IND1	7.57	6.12	7.57	7.63
DIR2	14.99	12.16	15.02	15.32
IND2	14.76	12.35	15.21	15.49
ΔRF (W m^{-2})				
DIR1-CONT	–3.91	–4.07	–4.85	–4.43
IND1-CONT	–7.02	–10.49	–10.52	–7.90
DIR2-CONT	–5.84	–6.97	–8.15	–7.06
IND2-CONT	–8.92	–12.83	–16.23	–10.92
Δr_e (μm)				
IND1-CONT	–2.52	–2.00	–2.37	–2.19
IND2-CONT	–2.77	–2.19	–2.63	–2.45
ΔT (K)				
DIR1-CONT	–0.51	–0.35	–0.25	–0.49
IND1-CONT	-0.79	–0.75	–0.55	–0.77
DIR2-CONT	–0.90	–0.70	–0.44	–0.76
IND2-CONT	–1.17	–1.12	–0.81	–1.14
ΔP (%)				
DIR1-CONT	–7.22	–4.43	3.15	–7.13
IND1-CONT	–14.56	–13.12	–9.09	–18.17
DIR2-CONT	–14.17	–10.44	–4.76	–15.04
IND2-CONT	–21.05	–18.23	–13.64	–25.42

during the spring transition season at a time when the source term is still relatively weak.

Note that the sulfate burden distribution shown in Figures 2a,b for the experiment IND1 is similar to that shown by GBQ02 for experiment CONT. Because of the effects of possible feedbacks induced by the aerosol forcing and because of the internal model variability (e.g., Giorgi and Bi, 2000), the aerosol burden generally varies in different simulations. However, as indicated by Tables I and II, these effects are relatively small so that the average sulfate burden is not very sensitive to the aerosol forcing and responds in a close to linear way to the sulfur emission. As a result, nearly doubled sulfate burden is found in correspondence of doubled sulfur emissions.

The indirect aerosol effects depend not only on the aerosol distribution, but also on cloudiness. Figure 3 compares the average cloud fractional cover over the region for DJF and JJA as simulated in the IND1 experiment with cloud cover observations from the dataset of New et al. (2000). The simulated total column fractional cloud cover is obtained from the daily averaged fractional cloudiness in each model layer (only daily averaged data were stored for these simulations) by using a random overlap approximation. Considering the uncertainty implied by this approximation the agreement between simulated and observed cloudiness is satisfactory.

The fractional cloud cover is minimum in DJF, when it varies from less than 30% in the north and northwest China regions to over 50% in central and south China. In DJF, the model underestimates cloudiness over the coastal regions of south China. Both in the simulation and in the observations, cloud cover is maximum during the summer monsoon season, when it varies from 40–50% in northwest China to over 70% in south and southwest China. In JJA the model overpredicts cloud cover over south China. Overall, however, the results of Figure 3 provide a picture of a realistic simulation of total cloudiness by the model.

A comparison of the spatial burden and cloudiness patterns in Figures 2 and 3 indicates that some areas of maximum sulfate concentration, in particular southwest and central China, are also characterized by relatively high cloud amounts. In addition, the seasonality of sulfate concentration, with a summer maximum and a winter minimum, is also similar to the seasonality of cloudiness. Both these results are not surprising in view of the fact that aqueous phase chemical conversion is the primary source of SO_4^{2-}. Therefore, the positive spatial and temporal correlation between cloudiness and sulfate concentration should tend to amplify the magnitude of the aerosol indirect effects.

3.1.1. *Aerosol Radiative Forcing*

Tables I and II report the regionally averaged top-of-the-atmosphere (TOA) radiative forcing due to the sulfate + soot aerosol in the DIR1 and IND1 experiments for the four seasons. The DIR1-CONT values measure the direct radiative forcing, while the IND1-CONT values also include the indirect effects. Note that the spatial

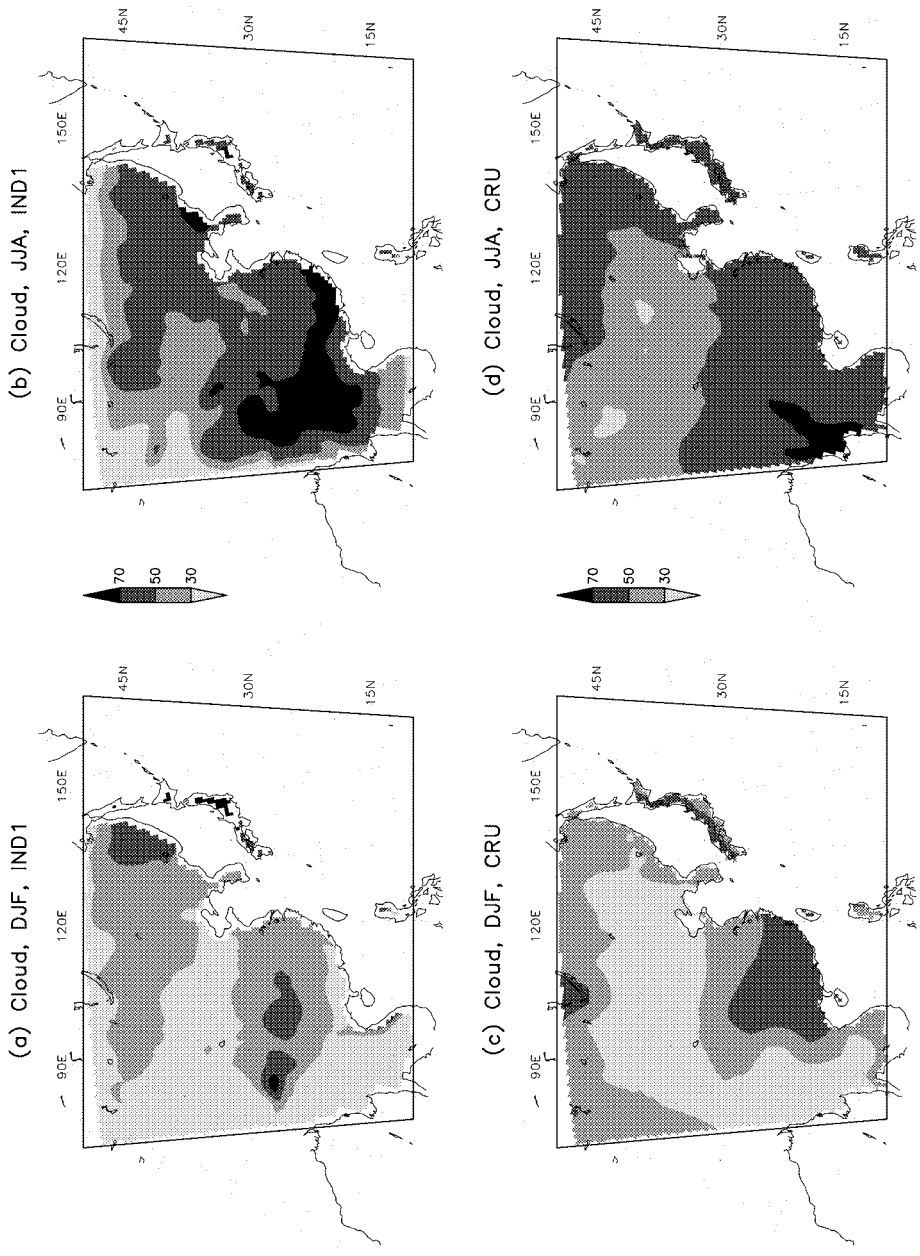

Figure 3. Simulated and observed average column fractional cloud cover over East Asia. (a) DJF, IND1 experiment; (b) JJA, IND1 experiment; (c) DJF, observations; (d) JJA, observations. Units are percentage of cloud cover. The observed values are from New et al. (2000).

structure of the direct radiative forcing essentially follows that of the aerosol burden (see GBQ02), with some modulation due to the cloud shading. The indirect forcing is more tied to the cloudiness, and thus it depends less on the aerosol burden and more on possible differences in cloud cover across experiments.

The direct radiative forcing shows a weak seasonal cycle in both regions, with a maximum in JJA or SON and a minimum in DJF, mostly in response to the weak seasonality of sulfate burden (see Tables I and II). Tables I and II show seasonally averaged TOA direct forcing values of –2.29 W m^{-2} to –2.74 W m^{-2} over east China and –3.91 W m^{-2} to –4.85 W m^{-2} over the Sichuan Basin. Local values of direct forcing are in the range of –1 W m^{-2} to –7 W m^{-2}. We should point out that these estimates include the effect of fossil fuel soot, which contributes a local positive radiative forcing in the range of 0.1–0.8 W m^{-2} (see GBQ02).

By contrast, the indirect forcing shows a very pronounced seasonality, especially when considering the whole east China region. In the IND1 experiment the total negative TOA radiative forcing varies from –3.93 W m^{-2} (DJF) to –11.77 W m^{-2} (JJA) over east China and –7.02 W m^{-2} (DJF) to –10.52 W m^{-2} (JJA) over the Sichuan Basin. Comparison of the radiative forcing in the DIR1 and IND1 experiments (Tables I and II) indicates that the direct radiative forcing is greater in DJF and SON, i.e., the colder and drier seasons, while the indirect forcing dominates in the warmer and wetter seasons of MAM and JJA. When compared to the indirect forcing, the direct forcing appears more important in the Sichuan Basin (where a strong maximum in sulfate burden is found) than in the whole east China region. This result is an indication of a relatively low sensitivity of the indirect forcing to the sulfate concentration for large sulfate amounts.

The negative indirect radiative forcing is caused by an increase in cloud reflectivity due to a decrease in cloud droplet effective radius (see Section 2). Tables I and II report the change in effective cloud droplet radius caused by the sulfate aerosol over the two regions in the experiments including the indirect forcing. This was calculated by vertically and temporally averaging the cloud effective droplet radius in cloudy grid points throughout the simulation. It can be seen that in the IND1 experiment the effective droplet radius decreases in the presence of the aerosol by values that on average range between 1.6 and 2.5 μm.

3.1.2. *Surface Air Temperature*

Figures 4 and 5 illustrate the surface temperature response to the direct and indirect aerosol forcing. The temperature difference is shown between the experiments DIR1 and CONT (DJF and JJA; Figures 4a,b), IND1 and DIR1 (DJF and JJA; Figures 4c,d), IND1 and CONT (all seasons; Figures 5a–d), respectively. The DIR1-CONT difference measures the effect of the direct forcing alone, the IND1-DIR1 difference measures the effect of the indirect forcing alone, while the IND1-CONT difference measures the combined effect of both forcings. Shading indicates areas where the temperature response is statistically significant at the 90% confidence level according to a two-tailed t-test. Corresponding regionally

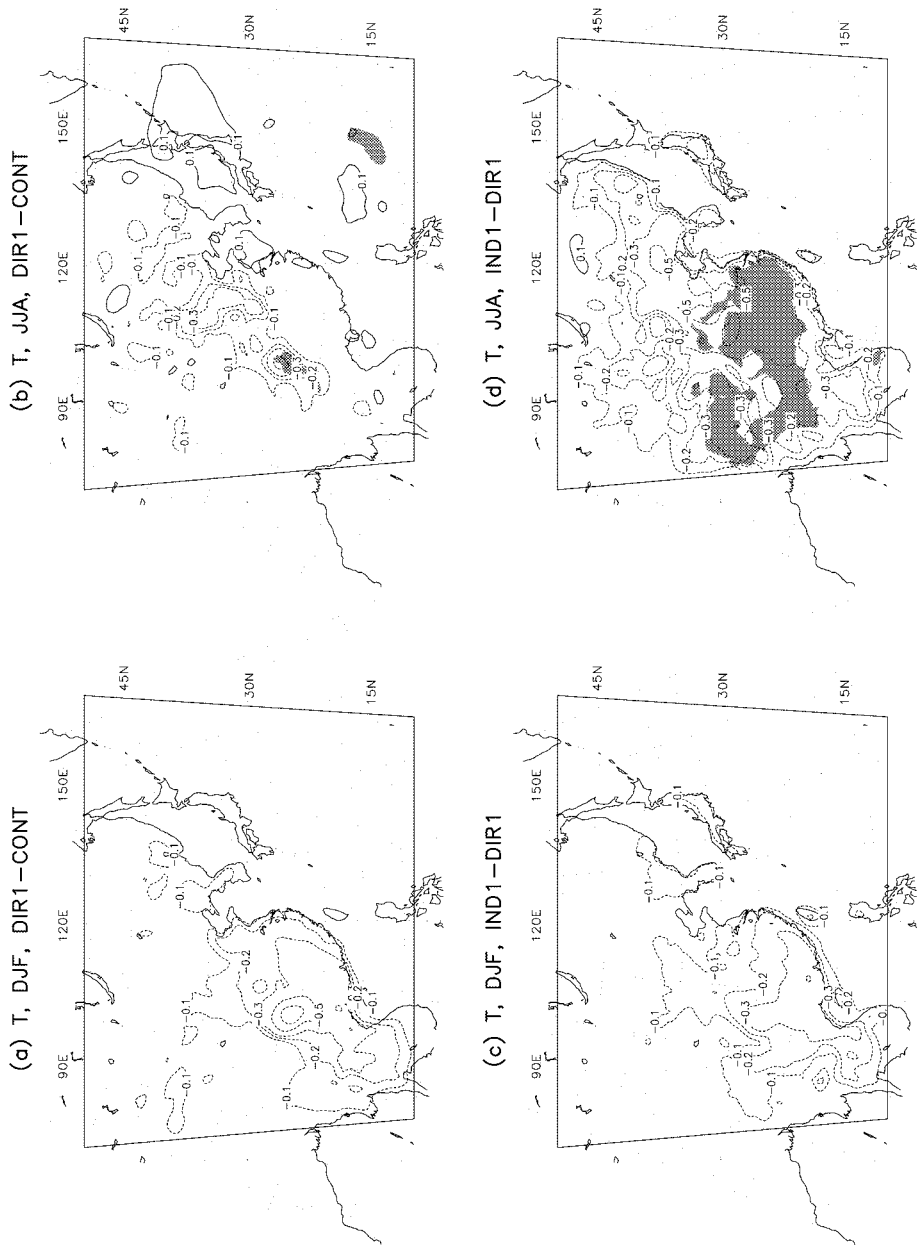

Figure 4. Difference in average seasonal surface air temperature between various experiments. (a) DIR1 minus CONT difference, DJF; (b) DIR1 minus CONT difference, JJA; (c) IND1 minus DIR1 difference, DJF; (d) IND1 minus DIR1 difference, JJA. Units are K. Shading indicates areas in which the difference is statistically significant at the 90% confidence level according to a two-tailed t-test.

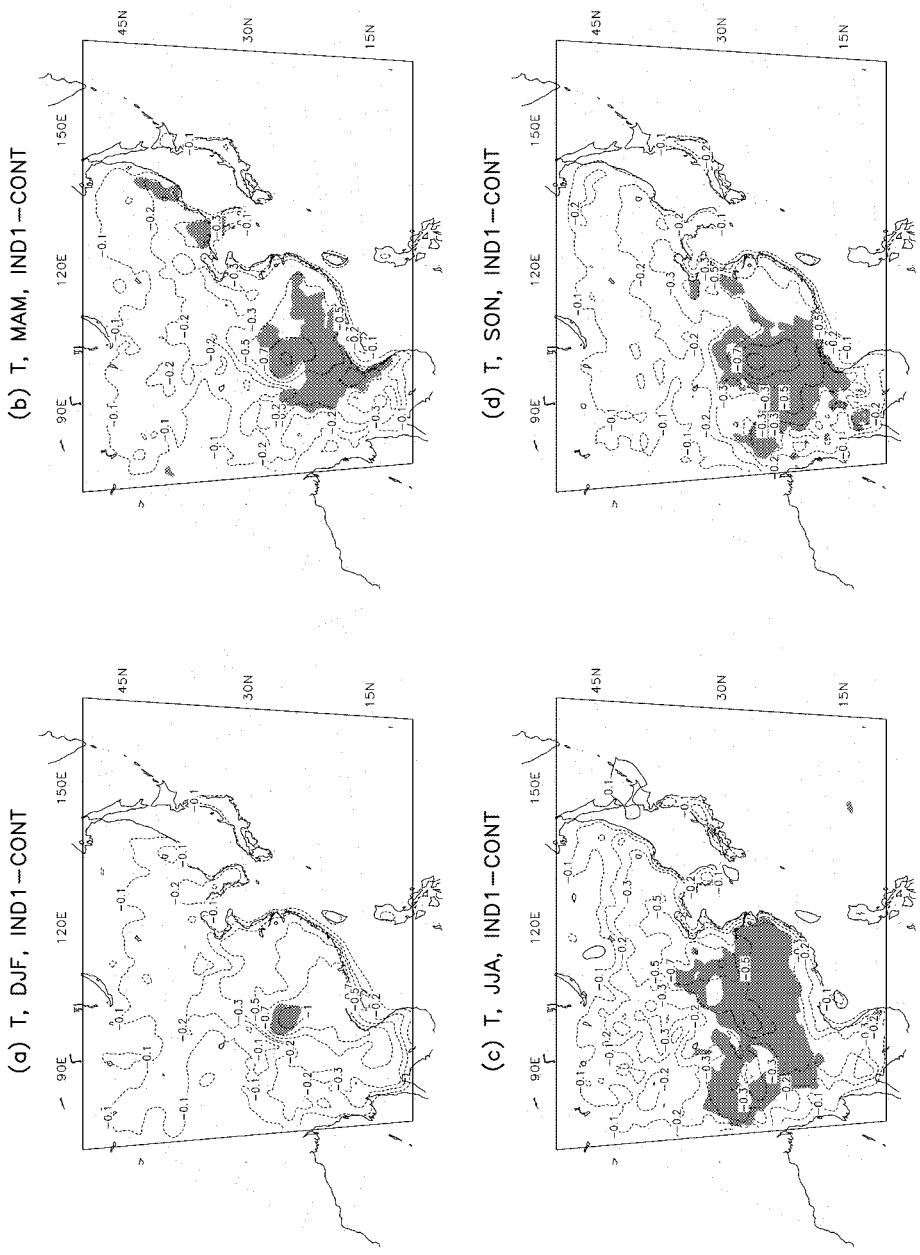

Figure 5. Difference in average seasonal surface air temperature between the IND1 and CONT experiments. (a) DJF; (b) MAM; (c) JJA; (d) SON. Units are K. Shading indicates areas in which the difference is statistically significant at the 90% confidence level according to a two-tailed t-test.

averaged temperature responses in the DIR1 and IND1 experiments are reported in Tables I and II. Note that in Table II the area average for the East China region only includes land points.

For the case of direct effects only (DIR1-CONT), surface cooling over east Asia land areas occurs in response to the negative direct aerosol radiative forcing in all seasons. The local cooling is in the range of –0.1 K to about –0.5 K, with a pronounced maximum over the Sichuan Basin in correspondence of the local maximum burden (see Figure 2). In DJF the cooling extends to most of east and south China, while in JJA it mostly extends from the Sichuan Basin towards the northeast China regions. However, only in the central regions of the Sichuan Basin in JJA the change is statistically significant.

As expected, the temperature response due to indirect forcing alone (IND1-DIR1) is more pronounced in JJA (–0.1 K to –0.6 K) than in DJF (–0.1 K to –0.3 K) because of the greater summer cloudiness. The indirect effect cooling does not show a marked maximum over the Sichuan Basin and, especially during the summer, it is much more widespread than the direct effect cooling. In fact, the indirect effect cooling is statistically significant over extended areas of east China in JJA, while it is still not significant in DJF.

The spatial distribution of the temperature response to the direct and indirect effects is quite different, especially in summer. This is because the direct effects depend on the aerosol distribution (Figure 2), while the indirect effects are mostly related to cloudiness (Figure 3). In JJA (Figure 2b) the region of maximum aerosol concentration extends from the Sichuan Basin towards northeast China, and the direct effect cooling shows a similar spatial pattern. Conversely, in JJA cloudiness is greater in south and central China than in north China (Figure 3b), and therefore the indirect effect cooling is more pronounced over south and central China. In DJF, the spatial patterns of aerosol and cloudiness are more similar, and so are the associated cooling patterns. Note that the model tends to overestimate cloudiness over south China in JJA and underestimate it in DJF (see Figure 2) and this can affect the simulated indirect effect cooling over the region.

When both direct and indirect effect forcings are combined (Figure 5), the maximum aerosol-induced surface cooling over the Sichuan Basin exceeds –1 K in DJF, MAM and SON, and –0.7 K in JJA. The cooling over the Sichuan Basin is mostly dominated by the direct effects. In JJA, cooling in excess of –0.7 K is found also over some regions of northeast China due to the contribution of both direct and indirect effects. In all seasons, most of east China experiences a cooling greater than –0.5 K. The cooling is statistically significant in all seasons over the Sichuan Basin, and it is significant over most of east and south China in JJA, MAM and SON. This latter feature is mostly attributable to the indirect aerosol forcing. Some regions of statistically significant cooling are also found over Korea and some northeast China coastal regions in MAM. The cooling is only of the order of a few tenths of a degree and not statistically significant over Japan.

Table III

Spatial correlation coefficient between the aerosol burden in the control experiment and the temperature difference between pairs of experiments. The correlation is calculated over the land regions of the interior of the domain

Experiments	DJF	MAM	JJA	SON
DIR1-CONT	0.88	0.77	0.37	0.87
IND1-CONT	0.87	0.80	0.51	0.86
IND1-DIR1	0.73	0.66	0.38	0.47
DIR2-CONT	0.91	0.88	0.62	0.92
IND2-CONT	0.90	0.86	0.61	0.89
IND2-DIR2	0.72	0.69	0.11	0.51

The average temperature response to the direct radiative forcing over the east China region is of the order of –0.07 K to –0.22 K (Table I). Over the Sichuan Basin (Table II) the average temperature response to the direct forcing is more than twice as large, –0.25 K to –0.51 K. As a result of the indirect radiative forcing, in the warm seasons the temperature response in the IND1 case is more than twice as large as in the DIR1 case, both for the whole of east China (–0.37 K to –0.42 K) and the Sichuan Basin (–0.55 K to –0.75 K). In the cold seasons, the average temperature response is about –0.39 K over east China and about –0.78 K over the Sichuan Basin, corresponding to an intensification of the cooling compared to the DIR1 case of about 85% for east China and 55% for the Sichuan Basin. Tables I and II thus indicate that the direct aerosol effect has a greater role in determining the surface cooling in the cold seasons, especially over the Sichuan Basin, while the indirect effects are dominant in the warm seasons.

It is interesting to note from Tables I and II that, both for the direct and indirect effects, the warm seasons (MAM and JJA) tend to show a less pronounced temperature response to the radiative forcing than the cold seasons (DJF and SON). Different factors can contribute to this result. In the warm seasons, greater cloudiness over China shields more effectively the surface from solar radiation and since the aerosol forcing occurs in the presence of solar radiation, this renders the surface less sensitive to a given aerosol forcing. In addition, in the warm season the surface hydrology has a greater influence on the surface temperature so that effects of the aerosol forcing on the hydrologic cycle (see next section) may in turn affect the surface temperature response.

Table III shows the spatial correlation coefficient between the temperature response in different forcing cases and the sulfate burden of the CONT run. The correlation is calculated over the area including all land points in the interior of the domain. This correlation is high, greater than 0.77, in DJF, MAM, and

SON both for the DIR1 and IND1 experiments, indicating a direct relationship between aerosol-induced forcing and surface temperature response. The correlation decreases substantially, values ≤ 0.51, during the summer in both cases. Evidently the more non-linear and random nature of summer convective precipitation and cloudiness tends to decouple the spatial structure of radiative forcing and temperature response, even though widespread aerosol-induced cooling is still produced. The correlation between temperature response and sulfate burden decreases in all seasons when only the indirect effects are considered (IND1-DIR1). This is because the indirect effects do not depend only on the aerosol distribution, but also on the distribution of cloudiness.

3.1.3. *Precipitation*

GBQ02 showed that the negative aerosol direct radiative forcing and subsequent surface cooling tend to inhibit precipitation because of increased atmospheric stability. In their experiments, however, the precipitation decrease was small and mostly not statistically significant. When also the indirect effect is added, the precipitation decrease is substantially more pronounced. Figures 6a–d present the IND1-CONT seasonal precipitation differences. The aerosol-induced precipitation decrease is evident in all seasons, and especially in JJA and SON, when the change is statistically significant over extended areas of China.

Tables I and II quantify the aerosol-induced precipitation changes over the east China and Sichuan Basin regions in the different experiments. An aerosol-induced decrease in precipitation occurs in all experiments and seasons except over the Sichuan Basin in the DIR1 JJA case. The precipitation decrease in the DIR1 experiment is most pronounced over the Sichuan Basin, with values of up to 7.2% of CONT precipitation. In the DIR1 case, the precipitation decrease is small, less than 6%, over the east China region in all seasons. Inclusion of the indirect effects substantially enhances the precipitation response in all seasons and regions, generally by factors greater than 2 compared to the DIR1 case. Over the Sichuan Basin the precipitation decrease reaches magnitudes of about 15–18% of CONT precipitation in DJF and SON and 9–13% in MAM and JJA. For the whole east China region, the precipitation decrease in the IND1 case is of the order of 5% to 13% of CONT precipitation across seasons. Overall, Tables I and II indicate that the indirect effects dominate in the generation of a negative precipitation response to the aerosol forcing. This is because the indirect effects are active in cloudy conditions while the direct effects are most effective in cloud-free conditions.

3.1.4. *Comparison with Observed Changes*

GBQ02 and Qian and Giorgi (2000) present an analysis of the observed surface air temperature record over China during the last several decades and show that several regions of central China, in particular the Sichuan Basin and regions of central-east China are characterized by a statistically significant cooling trend, most pronounced in the spring and summer seasons. As an example of this temperature

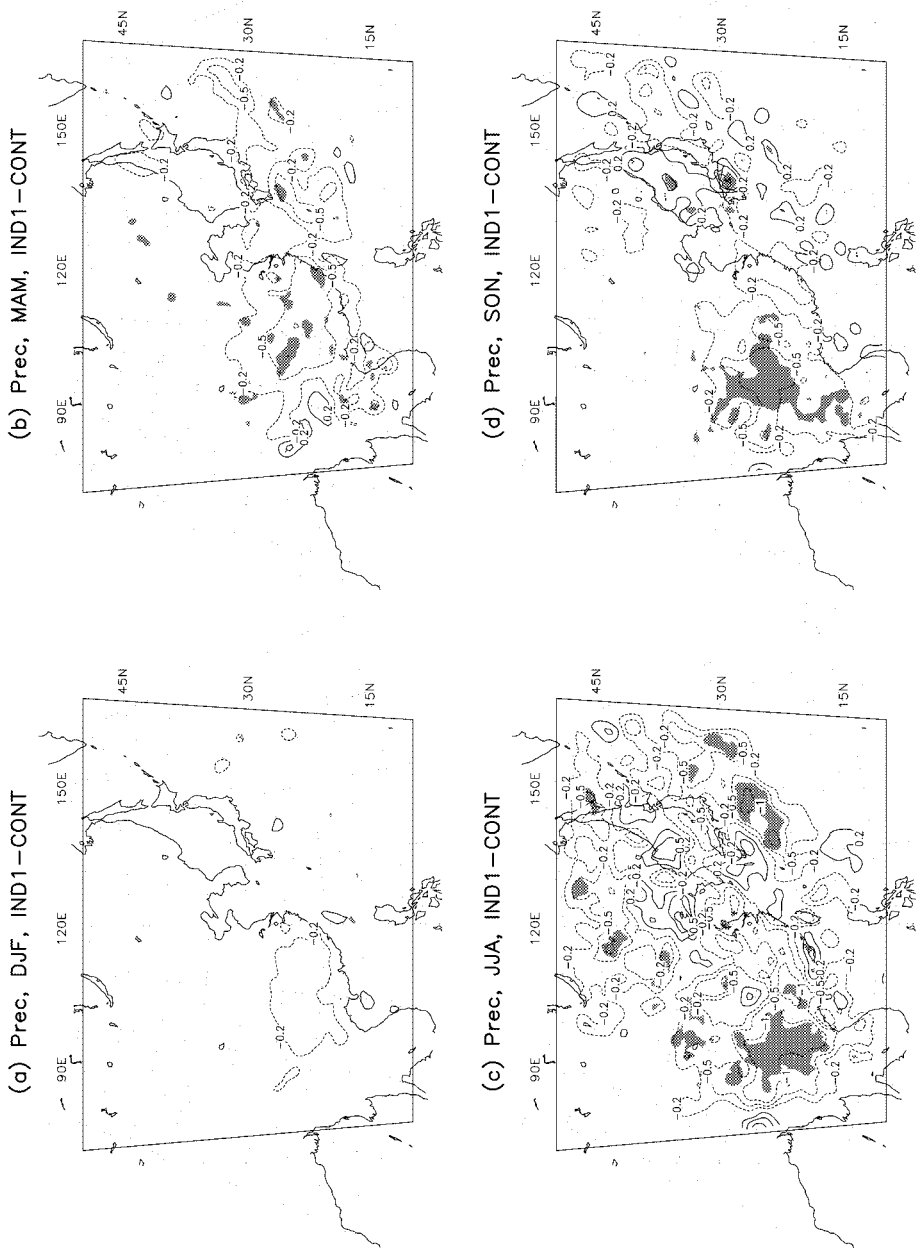

Figure 6. Difference in average seasonal precipitation between the IND1 and CONT experiments. (a) DJF; (b) MAM; (c) JJA; (d) SON. Units are mm day^{-1}. Shading indicates areas in which the difference is statistically significant at the 90% confidence level according to a two-tailed t-test.

trend, Figures 7a,b show the observed DJF and JJA temperature difference between the periods 1981–98 and 1951–80. These figures suggest that most of east Asia has undergone a large scale warming, especially in the cold season and at high latitudes. This warming, which is statistically significant over most regions, is consistent with the global warming observed in the latest decades of the the 20th century. On the other hand, some regions of east China, and in particular the Sichuan Basin, show cooling, which is statistically significant in the warm season over extended areas.

From an analysis of trends in aerosol optical depth, Qian and Giorgi (2000) hypothesize that the regional cooling trends implied by Figures 7a,b may be due to an increase in aerosol radiative forcing. It is difficult to separate the aerosol-induced signal from the underlying natural variability and greenhouse gas signal. However, when we consider that the aerosol effect over east China is likely superimposed to a large scale background warming, we can estimate from Figure 7 a possible aerosol-induced cooling effect of several tenths of a degree to over a degree over different regions of central and east China. As also noted by GBQ02, the cooling in the DIR1 experiment does not appear sufficient to explain the overall observed trend (see Figure 4), especially in the summer. However, as shown by Figure 5, the indirect aerosol effects substantially reinforce the direct effect cooling, especially in the summer. It thus appears that, when only present day sulfur emissions are considered, indirect effects are necessary to produce a surface temperature response comparable to that estimated from observations.

We also examined observed precipitation trends in East Asia over the last decades and found that they were generally small, of both signs and almost in no areas statistically significant at the 90% confidence level (not shown). Therefore, the simulated sulfate-induced precipitation decrease was not evident in the observed record. It is possible that the model overestimates the precipitation response to the sulfate-induced cooling, however, other factors can also explain this result. In reality the effect of sulfate on precipitation is embedded within the natural interannual to multi-decadal variability, which can mask the aerosol signal, and it is competing with the effects of other forcings. Among these are changes in large scale circulations due to greenhouse gas warming, land use and land cover changes and the effects of carbonaceous aerosols. Concerning the latter, since carbonaceous aerosols are good absorbers of solar radiation, they would also contribute to cool the surface. However they would heat up the lower troposphere, and as a result alter the vertical temperature profiles and thus the local hydrologic cycle. All these factors make the identification of a sulfate-induced precipitation signal in the observed record very difficult.

3.2. DOUBLED SULFUR EMISSION EXPERIMENTS

Tables I and II show that the response of the sulfate burden to the sulfur emission is nearly linear, with close to doubled sulfate amounts in correspondence of doubled emission. The sulfate burden in the DIR2 and IND2 cases (not shown) is also

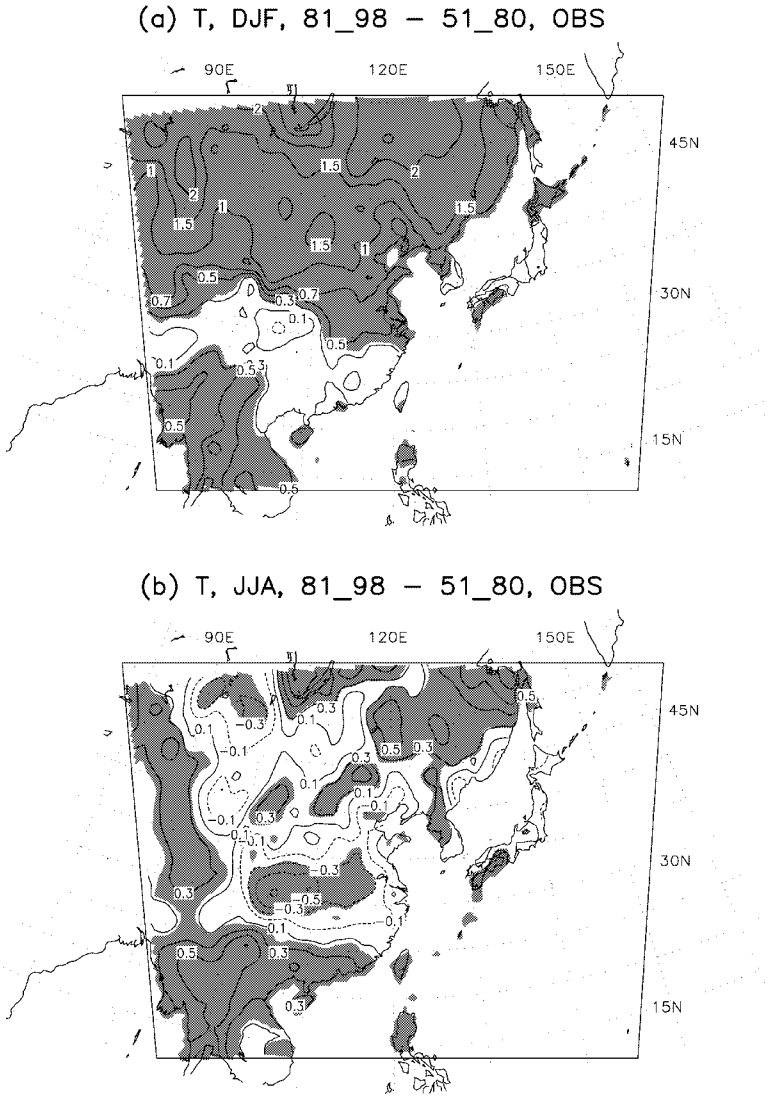

Figure 7. Difference in observed seasonal surface air temperature between the periods 1981–1998 and 1951–1980. (a) DJF; (b) JJA. Units are K. The data are from New et al. (2000). Shading indicates areas in which the difference is statistically significant at the 90% confidence level according to a two-tailed t-test.

characterized by a spatial structure similar to that of Figure 2, but with nearly doubled magnitude of values. The response of the direct radiative forcing to doubled emission is less than linear, especially in areas characterized by maximum aerosol loading, because of the exponential nature of the solar extinction by aerosols and because of the shading by clouds. This is illustrated by the average TOA radiative

forcing values of Tables I and II, which are less than twice as large in DIR2 than in DIR1, especially over the Sichuan Basin.

From Tables I and II, we can also calculate the average increase in TOA radiative forcing between the IND2 and DIR2 experiments, which measures the indirect effect forcing. When we compare these values with the differences between the IND1 and DIR1 forcings we find that they are generally comparable. This indicates that the increase in the indirect radiative forcing by doubling of the aerosol concentration is small. Indeed the decrease in cloud effective droplet radius from the IND1 to the IND2 experiment is also small, only a few tenths of μm in terms of temporal and vertical average (Tables I and II). As already mentioned, this behavior is due to the weak dependence of the droplet radius on the aerosol concentration for the large aerosol amounts found in our experiments. From the physical point of view, this result can be explained by the fact that, for a given amount of moisture, the number of particles that are activated to become CCN is limited, so that a further increase in aerosol amount does not lead to an increased CCN concentration.

Figures 8 and 9 show the following temperature differences: DIR2-CONT (DJF and JJA; Figures 8a,b), which measures the response to the direct effects only; IND2-DIR2 (DJF and JJA; Figures 8c,d), which measures the response to the indirect effects only; IND2-IND1 (DJF and JJA; Figures 8e,f), which measures the effect of doubling emission on the response; IND2-CONT (all seasons; Figures 9a,d), which measures the total combined response to both direct and indirect effects. The corresponding regional averages of the temperature responses are reported in Tables I and II.

When only the direct effects are included, doubling of the emission causes an increase of local surface cooling in the range of –0.1 K to –0.5 K (compare Figures 8a,b and 4a,b and see Tables I and II), and in the experiment DIR2 the cooling over the entire Sichuan Basin becomes statistically significant both in DJF and JJA. Table I shows that, when averaged over the entire east China region, the cooling in experiment DIR2 increases by a factor of about 1.5 in SON, 2 in MAM and DJF, and 3 in JJA, compared to the experiment DIR1. Over the Sichuan Basin the temperature response increases by a factor of 1.5 to 2. Despite these substantial increases, however, the magnitude of the direct-effect cooling remains small, less than 0.2 K over south and south-central China in JJA. Comparison of Figures 8c,d with Figures 4c,d also indicates that the cooling induced by the indirect effects is not sensitive to the doubling of aerosol concentration. This result, which is confirmed by Tables I and II, can be expected in view of the low sensitivity of the indirect effect radiative forcing to the aerosol amounts.

Figures 8e,f and 9a,d show the increase in cooling from IND1 to IND2 and the total temperature response in IND2, respectively. The increased cooling between IND1 and IND2 is of the order of –0.1 K to –0.5 K, and it is mostly due to the direct forcing component (see also Tables I and II). The total cooling in Exp. IND2 exceeds –1.5 K in the Sichuan Basin in DJF, MAM and SON, and –1 K in JJA. Over most of east China the cooling is in excess of –0.7 K in all seasons and it

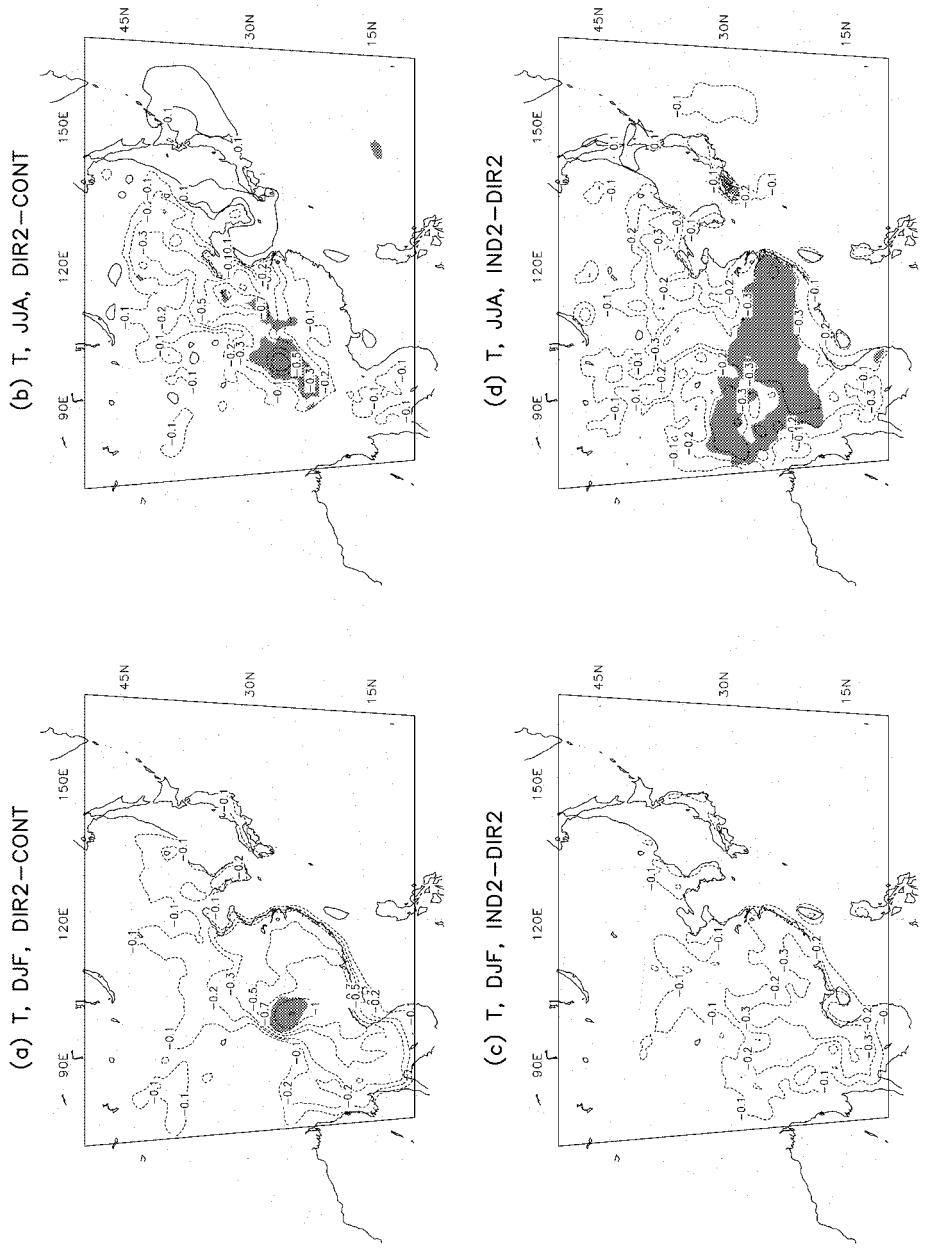
(a) T, DJF, DIR2−CONT
(b) T, JJA, DIR2−CONT
(c) T, DJF, IND2−DIR2
(d) T, JJA, IND2−DIR2
45N
30N
15N
90E
120E
150E

Figure 8a–d.

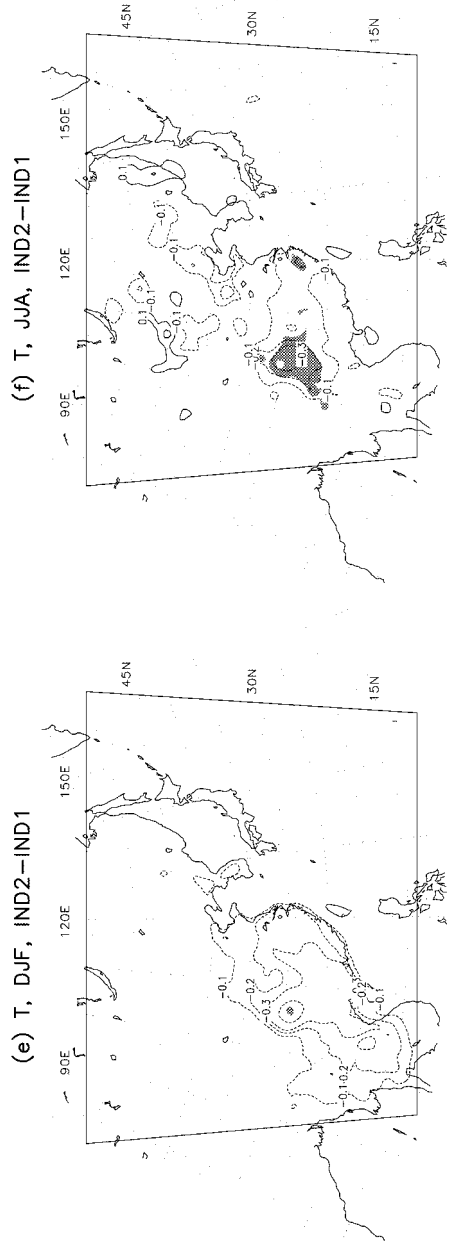

Figure 8e–f.

Figure 8. Difference in average seasonal surface air temperature between various experiments. (a) DIR2 minus CONT difference, DJF; (b) DIR2 minus CONT difference, JJA; (c) IND2 minus DIR2 difference, DJF; (d) IND2 minus DIR2 difference, JJA; (e) IND2 minus IND1 difference, DJF; (f) IND2 minus IND1 difference, JJA. Units are K. Shading indicates areas in which the difference is statistically significant at the 90% confidence level according to a two-tailed t-test.

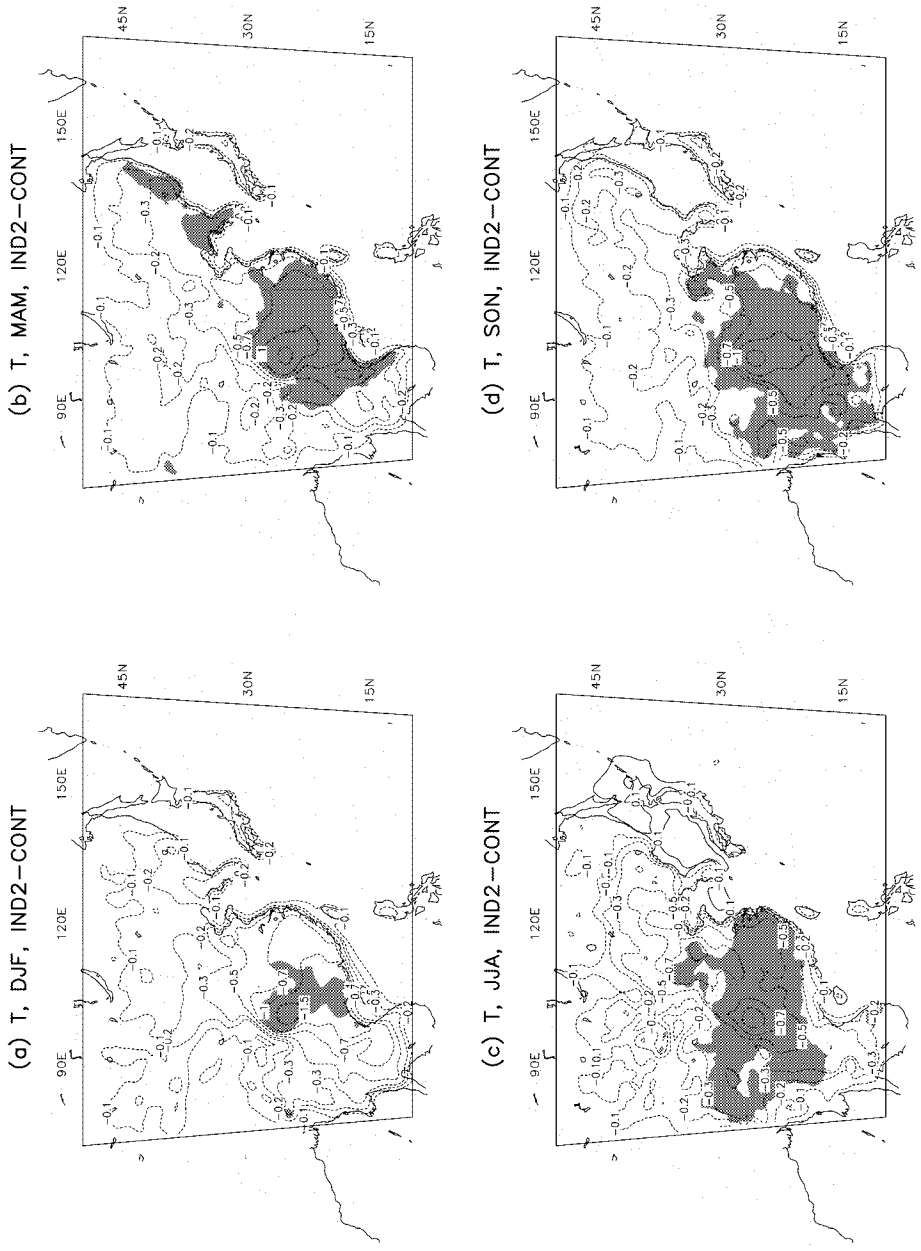

Figure 9. Difference in average seasonal surface air temperature between the IND2 and CONT experiments. (a) DJF; (b) MAM; (c) JJA; (d) SON. Units are K. Shading indicates areas in which the difference is statistically significant at the 90% confidence level according to a two-tailed t-test.

is statistically significant in MAM, JJA and SON. In DJF the area of statistically significant cooling is limited to the Sichuan Basin and regions to the east and south of it. Tables I and II show that, since the temperature response to the direct effects is more sensitive to the aerosol concentration than the response to the indirect effects, the contribution of the direct effects to the total cooling in the doubled emission experiments becomes dominant in all seasons except JJA.

Tables I and II also show the IND2-CONT seasonal and sub-regionally averaged precipitation changes. It is evident that the additional cooling caused by the higher sulfate concentrations in the DIR2 and IND2 runs further inhibits precipitation. The precipitation response is substantially enhanced in experiment DIR2 compared to DIR1 and when the indirect effects are added (IND2) the precipitation response is in the range of –13.6% (JJA) to –25.4% (SON) over the Sichuan Basin and in the range of –7.3% (JJA) to –16.6% (DJF) over the east China region. Compared to the IND1 experiment, in the IND2 experiment greater areas of statistically significant precipitation response are found (not shown). Note in Tables I and II that, because of their greater sensitivity to the aerosol amount, the direct effects provide the largest contribution to the precipitation response in the doubled emission cases except for JJA.

4. Conclusions

The primary conclusions of the sensitivity experiments analysed in this work can be summarized as follows:

1. In general, the surface climate impact of the indirect aerosol effects is in the same direction, and thus tends to reinforce, the impact of the direct effects. The radiative forcing of both direct and indirect aerosol effects is negative, which results in a cooling of the surface.
2. Under present day sulfur emissions, the direct aerosol radiative forcing is greater than the indirect forcing in the cold seasons, while the indirect forcing dominates in the warm seasons, when cloudiness is maximum.
3. Under present day sulfur emissions, the local surface temperature response due to direct aerosol effects is in the range of about –0.1 K to –0.7 K, with a marked maximum over the Sichuan Basin in response to a local maximum in aerosol burden. However, the surface cooling is statistically significant only over small regions. When indirect effects are included the surface cooling is more than doubled in the warm seasons (MAM and JJA) and substantially increased also in the cold seasons (SON and DJF). In the presence of the indirect effects the surface cooling can locally exceed –1 K and extended areas of statistically significant cooling are found in JJA, MAM and SON. The indirect effects dominate the surface cooling in MAM and JJA, while the direct effects prevail in DJF and SON.

4. The aerosol forcing tends to inhibit precipitation. Under present day sulfur emissions, this effect is essentially negligible when only the direct effects are included while it becomes much more pronounced, and in some areas statistically significant, when the indirect effects are added.
5. Doubling of the sulfur emissions leads to a substantial reinforcement of the direct effects, both in terms of radiative forcing and corresponding surface temperature and precipitation response. Conversely, the indirect effects show little sensitivity to doubling of the aerosol amounts. This has the important implication that while the direct effects can be expected to become increasingly important as the pollution emissions increase with future economic growth, the indirect effects may show an asymptotic behavior in foreseeable conditions. In fact, the present day aerosol amounts over the region may already be large enough that the indirect effects are close to their peak efficiency.
6. Overall, the indirect effects appear necessary to explain the observed temperature record over some regions of China, at least in the warm season.

In the assessment of our results it should be emphasized that a number of uncertainties are still present in both understanding and modeling of aerosol effects, especially the indirect ones. These uncertainties cover a range of aspects of the problem:

(i) Modeling of Type II indirect effects. In our model we have not addressed this issue, which is potentially an important one (e.g., Lohmann and Feichter, 1997), because of the relatively crude representation of cloud microphysics processes in our regional climate model and because of the lack of observational data to validate possible parameterizations of this process.

(ii) Description of the relationship between aerosol concentration and cloud optical properties. As mentioned, several empirical relationships are available in the literature, based on different observational studies, which yield different forcings (e.g., Jones and Slingo, 1996). It is difficult to objectively evaluate which one is most realistic over east Asia.

(iii) Representation of cloud processes. As is well known, the representation of cloud processes, both from the microphysical and macroscale points of view, is still one of the areas of greatest need of improvement in present day climate models.

(iv) Contribution of aerosols other than anthropogenic sulfate, which is likely important over the east Asia region. Both sulfate and carbonaceous aerosols shield the surface from solar radiation, and thus their effects on the surface temperature signal is in the same direction. However, while sulfate mostly reflects solar radiation back to space, carbonaceous aerosols absorb solar radiation and induce heating of the lower troposphere. The two types of aerosols may thus have a different impact on the hydrologic cycle, a feature that cannot be captured by the doubled sulfur emission experiment. The inclusion of

carbonaceous aerosol in the model is thus a high priority next step in model development.

(v) Our regional model simulations can only account for the local climatic impacts of the aerosol forcing, since possible feedbacks of this regional forcing onto the global circulation are not described. On the other hand, since we are using observed fields to drive the regional model, large scale circulation effects are already implicitly accounted for in the forcing fields.

All these elements contribute to the uncertainty in the estimate of the regional surface climate response to the aerosol forcing (e.g., Ramaswamy et al., 2001) and we plan to address them by further developing our coupled chemistry/aerosol-climate model. However, despite these uncertainties, our results strongly suggest that the radiative forcing due to both direct and indirect effects of anthropogenic aerosols has significantly influenced the surface climate of east Asia. It is therefore likely that if pollution emissions continue to increase along with the economic development of the region, anthropogenic aerosols will be an increasingly important factor in determining the climatic and environmental conditions of the region.

Acknowledgements

We thank the reviewers for their useful comments which helped to improve the quality of the paper. Yun Qian's participation was supported by the U.S. Department of Energy (DOE)'s Office of Science Biological and Environmental Research under a bilateral agreement between China Meteorological Administration and the U.S. DOE on climate change. The Pacific Northwest National Laboratory is operated for the U.S. DOE by Battelle Memorial Institute under Contract DE-AC06-76RLO1830.

References

Barrie, L. A., Yi, Y., Leaitch, W. R., Lohmann, U., Kasibhatla, P., Roelofs, G. J., Wilson, J., McGovern, F., Benkovitz, C., Melieres, M. A., Law, K., Prospero, J., Kritz, M., Bergmann, D., Bridgeman, C., Chin, M., Christensen, J., Easter, R., Feichter, J., Land, C., Jeuken, A., Kjellstrom, E., Koch, D., and Rasch, P. J.: 2000, 'A Comparison of Large Scale Atmospheric Sulfate Aerosol Models (COSAM): Overview and Highlights', *Tellus* **53B**, 615–645.

Boucher, O. and Lohmann, U.: 1995, 'The Sulfate-CCN-Cloud Albedo Effect: A Sensitivity Study with Two General Circulation Models', *Tellus* **47B**, 281–300.

Briegleb, B. P.: 1992, 'Delta–Eddington Approximation for Solar Radiation in the NCAR Community Climate Model', *J. Geophys. Res.* **97**, 7603–7612.

Chameides, W. L.: 1995, *The Yangtze Delta of China as an Evolving Metro-Agro-Plex. Proposal to the National Aeronautics and Space Administration*, Georgia Institute of Technology, Atlanta, Georgia, 80302, U.S.A., p. 55.

Chameides, W. L., Kasibhatla. P. S., Levy, H., and Moxim, W. J.: 1994, 'Growth of Continental Scale Metro-Agro-Plexes, Regional Ozone Pollution and World Food Production', *Science* **264**, 74–77.

Chameides, W. C., Li, X. S., Tao, X. Y., Zhou, X. J., Luo, C., Kiang, C. S., John, J. St., Saylor, R., Liu, S. C., Lam, K. S., Wang, T., and Giorgi, F.: 1999, 'Is Ozone Pollution Affecting Crop Yields in China?', *Geophys. Res. Lett.* **26**, 867–870.

Chameides, W. L., Liu, S. C., Yu, H. B., Bergin, M., Zhou, X. J., Mearns, L. O., Gao, W., Kiang, C. S., Saylor, R. D., Luo, C., Huang, Y., Steiner, A., and Giorgi, F.: 1999, 'A Case Study of the Effects of Atmospheric Aerosols and Regional Haze on Agriculture: An Opportunity to Enhance Crop Yields in China through Emission Controls?', *Proceedings of the National Academy of Sciences* **96**, 13626–13633.

Charlson, R. J., Langner, J., and Rodhe, H.: 1990, 'Sulphate Aerosols and Climate', *Nature* **348**, 22.

Charlson, R. J., Schwartz, S. E., Hales, J. M., Coakley, R. D., Hansen, J. E., and Hoffman, D. J.: 1992, 'Climate Forcing by Anthropogenic Aerosols', *Science* **255**, 423–430.

Giorgi, F.: 1989, 'Two-Dimensional Simulations of Possible Mesoscale Effects Nuclear War Fires. I: Model Description', *J. Geophys. Res.* **94**, 1127–1144.

Giorgi, F. and Bi, X. Q.: 2000, 'A Study of Internal Variability of a Regional Climate Model', *J. Geophys. Res.* **105**, 29503–29521.

Giorgi, F., Bi, X. Q., and Qian, Y.: 2000, 'Direct Radiative Forcing and Regional Climatic Effects of Anthropogenic Aerosols over East Asia: A Regional Coupled Climate-Chemistry/Aerosol Model Study', *J. Geophys. Res.* **107** (D20), 4439, doi: 10.1029/2001JD001066.

Giorgi, F. and Chameides, W. L.: 1986, 'Rainout Lifetimes of Highly Soluble Aerosols', *J. Geophys. Res.* **91**, 14367–14376.

Giorgi, F., Huang, Y., Nishizawa, K., and Fu, C. B.: 1999, 'A Seasonal Cycle Simulation over Eastern Asia and its Sensitivity to Radiative Transfer and Surface Processes', *J. Geophys. Res.* **104**, 6403–6423.

Giorgi, F., Marinucci, M. R., and Bates, G. T.: 1993, 'Development of a Second Generation Regional Climate Model (RegCM2). Part I: Boundary-Layer and Radiative Transfer Processes', *Mon. Wea. Rev.* **121**, 2794–2813.

Giorgi, F., Marinucci, M. R., Bates, G. T., and De Canio, G.: 1993, 'Development of a Second Generation Regional Climate Model (RegCM2). Part II: Convective Processes and Assimilation of Lateral Boundary Conditions', *Mon. Wea. Rev.* **121**, 2814–2832.

Giorgi, F. and Shields, C.: 1999, 'Tests of Precipitation Parameterizations Available in the Latest Version of the NCAR Regional Climate Model (RegCM) over Continental U.S', *J. Geophys. Res.* **104**, 6353–6375.

Haywood, J. M. and Boucher, O.: 2000, 'Estimates of the Direct and Indirect Radiative Forcing Due to Tropospheric Aerosols: A Review', *Rev. Geo.* **38**, 513–543.

Haywood, J. M., Roberts, D. L., Slingo, A., Edwards, J. M., and Shine, K. P.: 1997, 'General Circulation Model Calculations of the Direct Radiative Forcing by Anthropogenic Sulfate and Fossil-Fuel Soot Aerosol', *J. Climate* **10**, 1562–1577.

Haywood, J. M. and Shine, K. P.: 1997, 'Multi-Spectral Calculations of the Direct Radiative Forcing of Tropospheric Sulphate and Soot Aerosols Using a Column Model', *Quart. J. R. Meteorol. Soc.* **123**, 1907–1930.

Hegg, D. A.: 1994, 'Cloud Condensation Nucleus-Sulfate Mass Relationship and Cloud Albedo', *J. Geophys. Res.* **99**, 25,903–25,907.

Jones, A., Roberts, D. L., and Slingo, A.: 1994, 'A Climate Model Study of Indirect Radiative Forcing by Anthropogenic Sulphate Aerosols', *Nature* **370**, 450–453.

Jones, A. and Slingo, A.: 1996, 'Predicting Cloud-Droplet Effective Radius and Indirect Sulphate Aerosol Forcing Using a General Circulation Model', *Quart. J. Roy. Meteorol. Soc.* **122**, 1573–1595.

Kasibhatla, P., Chameides, W. L., and John, J. St.: 1997, 'A Three-Dimensional Global Model Investigation of Seasonal Variation in the Atmospheric Burden of Anthropogenic Sulfate Aerosols', *J. Geophys. Res.* **102**, 3737–3759.

Kiehl, J. T. and Briegleb, B. P.: 1993, 'The Relative Role of Sulfate Aerosols and Greenhouse Gases in Climate Forcing', *Science* **260**, 311–314.

Kiehl, J. T., Hack, J. J., Bonan, G. B., Boville, B. A., Briegleb, B. P., Williamson, D. L., and Rasch, P. J.: 1996, 'Description of the NCAR Community Climate Model (CCM3)', *NCAR Technical Note, NCAR/TN-420 + STR*, p. 152.

Kiehl, J. T., Schneider, T. L., Rasch, P. J., Barth, M. C., and Wong, J.: 2000, 'Radiative Forcing Due to Sulfate Aerosols from Simulations with the National Center for Atmospheric Research Community Climate Model', *J. Geophys. Res.* **105**, 1441–1457.

Liousse, C., Penner, J. E., Chuang, C., Walton, J. J., Eddleman, H., and Cachier, H.: 1996, 'A Global Three-Dimensional Model Study of Carbonaceous Aerosols', *J. Geophys. Res.* **101**, 19411–19432.

Lohmann, U. and Feichter, J.: 1997, 'Impact of Sulfate Aerosols on Albedo and Lifetime of Clouds: A Sensitivity Study with the ECHAM4 GCM', *J. Geophys. Res.* **102**, 13685–13700.

Luo, C., St. John, J. C., Zhou, X. J., Lam, K. S., Wang, T., and Chameides, W. L.: 2000, 'A Nonurban Ozone Air Pollution Episode over Eastern China: Observations and Model Simulations', *J. Geophys. Res.* **105**, 1889–1908.

Martin, G. M., Johnson, D. W., and Spice, A.: 1994, 'The Measurements and Parameterization of Effective Radius of Droplets in Warm Stratocumulus Clouds', *J. Atmos. Sci.* **51**, 1823–1842.

Myhre, G., Stordal, F., Restad, K., and Isaksen, I. S. A.: 1998, 'Estimation of the Direct Radiative Forcing Due to Sulfate and SSO Aerosols', *Tellus* **50B**, 463–477.

New, M. G., Hulme, M., and Jones, P. D.: 2000, 'Representing Twentieth-Century Space Time Climate Fields. Part II: Development of a 1901–1996 Mean Monthly Terrestrial Climatology', *J. Climate* **13**, 2217–2238.

Penner, J. E., Charlson, R. J., Hales, J. M., Laulainen, N. S., Leifer, R., Novakov, T., Ogren, J., Radke, L. F., Schwartz, S. E., and Travis, L.: 1994, 'Quantifying and Minimizing Uncertainty of Climate Forcing by Anthropogrnic Aerosols', *Bull. Amer. Meteorol. Soc.* **75**, 375–400.

Penner, J. E., Andreae, M., Annegarn, H., Barrie, L., Feichter, J., Hegg, D., Jarayaman, A., Leaitch, R., Murphy, D., Nganga, J., and Pitari, G.: 2001, 'Aerosols, their Direct and Indirect Effects', Chapter 5 of Houghton, J. T., Ding, Y. H., Griggs, D. J., Noguer, M., van der Linden, P. J., and Dai, X. X. (eds.), *Climate Change 2001; The Scientific Basis*, Contribution of Working Group I to the Third Assessment Report of the Intergovernmental Panel on Climate Change (IPCC), Cambridge University Press, Cambridge, U.K.

Qian, Y., Fu, C. B., and Wang, S. Y.: 1999, 'Mineral Dust and Climate Change', *Adv. Earth Sci.* **14**, 391–394 (in Chinese).

Qian, Y. and Giorgi, F.: 1999, 'Interactive Coupling of Regional Climate and Sulfate Aerosol Models over Eastern Asia', *J. Geophys. Res.* **104**, 6477–6499.

Qian, Y. and Giorgi, F.: 2000, 'Regional Climatic Effects of Anthropogenic Aerosols? The Case of Southwestern China', *Geophys. Res. Lett.* **27**, 3521–3524.

Qian, Y., Giorgi, F., Huang, Y., Chameides, W. L., and Luo, C.: 2001, 'Simulation of Anthropogenic Sulfur over East Asia with a Regional Coupled Chemistry-Climate Model', *Tellus* **53B**, 171–191.

Ramaswamy, V., Boucher, O., Haigh, J., Hauglustaine, D., Haywood, J., Myhre, G., Nkajima, T., Shi, G. Y., and Solomon, S.: 2001, 'Radiative Forcing of Climate Change', Chapter 6 of Houghton, J. T., Ding, Y. H., Griggs, D. J., Noguer, M., van der Linden, P. J., and Dai, X. X. (eds.), *Climate Change 2001: The Scientific Basis*, Contribution of Working Group I to the Third Assessment Report of the Intergovernmental Panel on Climate Change (IPCC), Cambridge University Press, Cambridge, U.K.

Smith, S. J., Pitcher, H., and Wigley, T. M. L.: 2001, 'Global and Regional Anthropogenic Sulfur Dioxide Emissions', *Global Planet. Change* **29**, 99–119.

Streets, D. G. and Waldhoff, S. T.: 2000, 'Present and Future Emissions of Air Pollutants in China: SO_2, NO_x, and CO', *Atmos. Environ.* **34**, 363–374.

Twomey, S. A., Piepgrass, M., and Wolfe, T. L.: 1984, 'An Assessment of the Impact of Pollution on Global Cloud Albedo', *Tellus* **36B**, 356–366.

Wang, W. X.: 1997, 'The Issue of Environmental Acidification in China', *Acta Scientiae Circumstantiae* **17**, 15–23 (in Chinese).

Wigley, T. M. L.: 1989, 'Possible Climate Change Due to SO_2 Derived Cloud Condensation Nuclei', *Nature* **339**, 365–367.

(Received 18 March 2002; in revised form 5 November 2002)